Algorithms to Estimate the Temperature and Effective Irradiance Level over a Photovoltaic Module using the Fixed Point Theorem

Eduardo I. Ortiz Rivera, *IEEE Student Member* and Fang Z. Peng, *IEEE Fellow*
Department of Electrical and Computer Engineering
Michigan State University
East Lansing, Michigan 48823
Email: ortizedu@egr.msu.edu

***Abstract*— The purpose of this paper is to present four algorithms to calculate the effective irradiance level, E_i and temperature, T, of operation for a photovoltaic module, PVM. The main reasons to develop these algorithms are for monitoring climate conditions, the elimination of temperature and solar irradiance sensors, reductions in cost for a photovoltaic inverter system, and development of new algorithms to be integrated with maximum power point tracking algorithms. The first three algorithms use only the short circuit current, open circuit voltage, the operating current and voltage for the PVM, avoiding the use of pyranometers and thermocouples. The last algorithm can estimate the irradiance level using only the open circuit voltage and the PVM temperature of operation. Finally, simulations and experimental results are presented in the paper.**

I. Introduction

The environmental conditions are an important factor in the performance of any photovoltaic module, PVM. An accurate measurement of the temperature, T and effective irradiance level, E_i is needed to improve the design of PV power systems and maximum power point tracking, MPPT algorithms. Also, the measured data is useful for online PV system characterization [1], [2], reliability of the weather conditions and meteorological data collection on a long term basis [3]. Also, with the measured data, it will be possible to determine if a PV system is cost/effective [4] and to predict the annual energy production for a PVM in a specific geographic region [5].

The typical sensor used to measure the solar irradiance over a PVM is a pyranometer [6]. A pyranometer is defined as an instrument for measuring the solar radiation and diffuse sky radiation, i.e. effective irradiance, on a plane surface [7]. Typically, pyronometers are used in terrestrial and space applications [2], [3], [4], [5], [6], [7], [8], [9], [10], [11], [12], [13]. Usually, for a low cost pyranometer a reasonable accuracy should be $\pm 5\%$ and for a high cost pyranometer a reasonable accuracy should be $\pm 2\%$ [8], [9]. Disadvantages with a pyranometer are that usually the price can be between 300 U.S. dollars and 1,800 U.S. dollars [9], the sensitivity may change with time and exposure to radiation [5], long periods of high temperature ($> 50^{\circ}C$) can damage the accuracy of the instrument [7] and often the pyranometers need to be calibrated every day whenever there is significant change in the weather conditions [7].

In addition to the solar irradiance, the temperature can affect the output of a PVM. The average temperature for a PVM should be measured using multiple thermocouples attached to the rear surface [14]. As advantages, the thermocouples can measure a wide range of temperatures and are cheap and standard devices in the industry [15]. Thermocouples in photovoltaic applications are used mainly for safety reasons monitoring the average temperature variations in a PVM [7]. The main disadvantages using thermocouples are limitations in the range of accuracy, noise, connection problems, decalibration [15] and the positioning over the surface of the PVM, where it can affect the PVM performance, or under the PVM, where inaccurate measurements of the PVM temperature could be obtained [14].

To avoid the use of sensors and to solve the problems exposed before, this paper proposes several Fixed-Point Iteration, FPI, algorithms using voltage and current measurements to calculate T and E_i over a PVM. These algorithms can be integrated with other algorithms related to MPPT (e.g. Linear Reoriented Coordinates Method, LRCM [16]) or to monitor the PVM performance [1]. The PVM mathematical model is described in the paper, and it is based on the manufacturer data sheets [2]. Finally, this paper describes the algorithms and compares the algorithms results to the measured results.

II. Photovoltaic Exponential Model

The PVM model to be used in this paper is described in (1), (2), (3) and (4). This PVM model describes the relationship of the current with respect to the voltage, effective irradiance level, E_i and temperature, T of operation for the PVM [17]. The main advantage of the given PVM model is that for any photovoltaic module, it can be described in terms of the values provided by the manufacturer data sheet and the standard test conditions [17].

The variables P, I and V are the photovoltaic module output power, current and voltage. I_{sc} is the short-circuit current at $25^{\circ}C$ and $1000W/m^2$. V_{oc} is the open-circuit voltage at $25^{\circ}C$ and $1000W/m^2$. V_{max} is the open-circuit voltage at $25^{\circ}C$ and more than $1,200W/m^2$, (usually, V_{max} is close to

$1.03 \cdot V_{oc}$). V_{min} is the open-circuit voltage at $25^{\circ}C$ and less than $200W/m^2$, (usually, V_{min} is close to $0.85 \cdot V_{oc}$). T_N is the nominal temperature, $25^{\circ}C$. E_{iN} is the nominal effective solar irradiation, $1,000W/m^2$. TCi is the temperature coefficient of I_{sc}, $(A/^{\circ}C)$. TCV is the temperature coefficient of V_{oc}, $(V/^{\circ}C)$. b is the characteristic constant for the PVM based on the I-V Curve. Vx is the open circuit voltage at any given E_i and T, and it is the voltage of operation for the PVM when the current, I is zero (2). Ix is the short circuit current at any given E_i and T, and it can be calculated from (3) when the voltage, V is zero.

Also, the power produced by the PVM can be calculated by multiplying I by V as given in (4). Finally, after substituting (2) and (3) on (1) and (4), the final relationship between P, I, V, T and E_i can be obtained.

$$I(V) = \frac{Ix}{1 - exp\left(\frac{-1}{b}\right)} \cdot \left[1 - exp\left(\frac{V}{b \cdot Vx} - \frac{1}{b}\right)\right] \quad (1)$$

$$\begin{aligned} Vx &= \frac{E_i}{E_{iN}} \cdot TCV \cdot (T - T_N) + V_{max} - (V_{max} - V_{min}) \\ &\cdot exp\left(\frac{E_i}{E_{iN}} \cdot ln\left(\frac{V_{max} - V_{oc}}{V_{max} - V_{min}}\right)\right) \end{aligned} \quad (2)$$

$$Ix = \frac{E_i}{E_{iN}} \cdot I_{sc} + TCi \cdot (T - T_N) \quad (3)$$

$$P(V) = \frac{V \cdot Ix}{1 - exp\left(\frac{-1}{b}\right)} \cdot \left[1 - exp\left(\frac{V}{b \cdot Vx} - \frac{1}{b}\right)\right] \quad (4)$$

III. Algorithms to Estimate the Effective Irradiance Level and Temperature of Operation for a PVM

To understand the proposed algorithms and their validity, the following paragraphs will explain the definition and theorems related to Fixed-Point Iteration, FPI and their relationship with the PVM mathematical model. A fixed point is defined as a number x such that x is the solution of $x = g(x)$ [18]. *Theorem 5.1* and *Theorem 5.2* are the basis for the conditions of existence and uniqueness for the proposed algorithms.

Theorem 1 (*Fixed Point Existence*): Assume that $g(x)$ is continuous on $[a, b]$, and that $a \leq$ g(x) $\leq b \; \forall \; x \in [a, b]$ then $\exists$ a fixed-point c in $[a, b]$. Due space limitations, the proof is not shown but it can be found in [18].

Theorem 2 (*Fixed Point Uniqueness*): Assume that $g(x)$ satisfies *Theorem 1*, $\partial g(x)/\partial x$ is continuous on (a, b) and $\exists$ a positive constant $P < 1$ where $|g'(x)| \leq P$, then $g(x)$ has a unique fixed point c on (a, b). The proof is in [18]. *Theorem 2* is also known as the *Contraction Mapping Theorem*.

For additional FPI theorems, definitions and applications please refer to [18], [19] and [20]. Now the proposed algorithms will be presented with their descriptions and applications.

Algorithm: 1. Fixed-Point Iteration to calculate T and E_i given Vx, V_1 and I_1. The algorithm considers the data provided by the PVM data sheet. Figure 1 shows the flowchart for *Algorithm 1*. The first step is to calculate Ix using (5). The second step is to iterate (6) and (7) to calculate T and E_i using T_N and E_{iN} as initial conditions.

$$Ix = \frac{I_1 - I_1 \cdot exp\left(\frac{-1}{b}\right)}{1 - exp\left(\frac{V_1}{b \cdot Vx} - \frac{1}{b}\right)} \quad (5)$$

$$\begin{aligned} T(n+1) &= T_N + \frac{E_i(n) \cdot (Vx - V_{max})}{TCV \cdot E_{iN}} \\ &+ \frac{E_i(n)}{TCV \cdot E_{iN}} \cdot (V_{max} - V_{min}) \\ &\cdot exp\left(\frac{E_i}{E_{iN}} \cdot ln\left(\frac{V_{max} - V_{oc}}{V_{max} - V_{min}}\right)\right) \end{aligned} \quad (6)$$

$$E_i(n+1) = \frac{Ix \cdot E_{iN}}{I_{sc} + TCi \cdot (T(n) - T_N)} \quad (7)$$

Figure 2 presents an integrated PVM converter system using a DSP Board to control the maximum power to the load and to calculate T and E_{iN} without pyranometers or thermocouples. *Algorithm 1* is programmed to the DSP Board. Finally, the proposed algorithm is able to find a unique solution for the effective irradiance level and temperature of operation over a PVM because (6) and (7) satisfy *Theorem 1* and *Theorem 2*.

Algorithm: 2. This fixed iteration algorithm considers the use of Ix and Vx to calculate T and E_{iN}. First, *Algorithm 2* reads Ix and Vx then iterates (6) and (7) as presented on the *Algorithm 1* description.

Algorithm: 3. Fixed-Point Iteration to Calculate T and E_i given V_1, V_2, I_1 and I_2. *Algorithm 3* is designed for a variable load with faster dynamics than T and E_i dynamics. The basic principle for *Algorithm 3* is the following: if the power in the load is changing but T and E_i are constants then the new operation point (V_2, I_2) will remain in the same I-V curve as the old operation point (V_1, I_1); hence, it is possible to calculate T and E_i. Figure 3 shows the flowchart for *Algorithm 3* where the first step is to read V_1, V_2, I_1 and I_2, as an initial value, $Vx(1)$ is equal to V_2 then iterate (8) and (9) to calculate Ix and Vx. Finally, Vx and Ix are sent to *Algorithm 2* to calculate T and E_i.

$$Ix(n+1) = \frac{I_1 - I_1 \cdot exp\left(\frac{-1}{b}\right)}{1 - exp\left(\frac{V_1}{b \cdot Vx(n)} - \frac{1}{b}\right)} \quad (8)$$

$$Vx(n+1) = \frac{V_1}{1 + b \cdot ln\left[1 - \frac{I_1}{I_2} + \frac{I_1}{I_2} \cdot exp\left(\frac{V_2}{b \cdot Vx(n)} - \frac{1}{b}\right)\right]} \quad (9)$$

Algorithm: 4. Fixed-Point Iteration to calculate E_i and Ix given Vx, and T. *Algorithm 4* is designed using the fact that the thermocouples are cheap. Hence using one sensor for the open circuit voltage, it is possible to calculate E_i. The algorithm reads T and Vx then iterates (10) to find E_i.

$$E_i(n+1) = \frac{(T - T_N) \cdot TCV \cdot E_{iN}}{Vx - V_{max} + (V_{max} - V_{min}) \cdot \left(\frac{V_{max} - V_{oc}}{V_{max} - V_{min}}\right)^{\frac{E_i(n)}{E_{iN}}}} \quad (10)$$

Finally, the proposed algorithms are valid to calculate T and E_i because *Theorem 1* and *Theorem 2* are satisfied due the

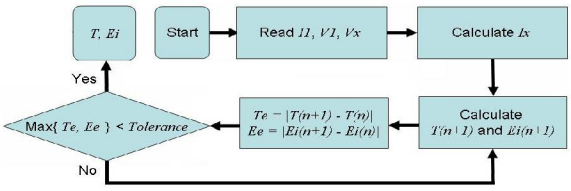

Fig. 1. Flowchart for *Algorithm 1* to calculate T and E_i.

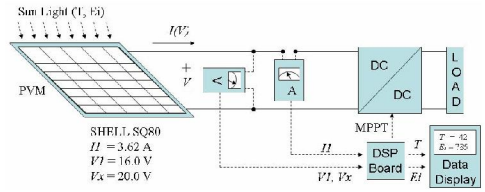

Fig. 2. Integrated PVM converter system, using a DSP Board programmed with the *Algorithm 1*.

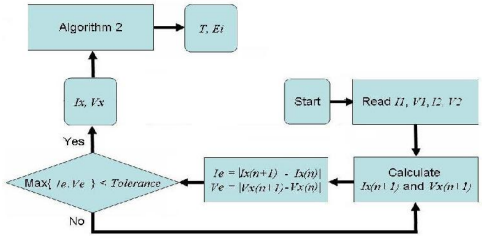

Fig. 3. Flowchart for *Algorithm 3* to calculate Ix and Vx, integrated with *Algorithm 2*.

continuity of the functions and partial derivatives of (6)-(10). As an advantage, the proposed algorithms can be integrated with other algorithms or methods with MPPT without affecting the performance of the PVM.

IV. Experimental Results

The electric specifications for four PVM (Table I and Table II) were used to validate and test the proposed algorithms. Figure 1 shows an integrated PV converter system where *Algorithm 1* and *Algorithm 2* were tested. Table III and Table V show the measured and expected parameters for the four PVM's using using *Algorithm 1* and *Algorithm 2* respectively. The results for the *Algorithm 1* and *Algorithm 2* are given in the Table IV and Table VI respectively. The number of iterations required to calculate T and E_i were less than 5 for both algorithms. The maximum relative error to approximate E_i is less than 3% and the maximum absolute error between the measured T and the calculated T was only $\pm 6^{\circ}C$, showing a good performance.

Also, the algorithms converge very fast with a good performance with the uniqueness property presented in *Theorem 2*. The LRCM [16] was integrated with *Algorithm 2* to approximate the maximum power produced by the PVM's on real time conditions, *Pap* as shown in Table VI. Finally, these algorithms can track the meteorological conditions for a long term because the collected data can be stored and recorded without interfering with the PVM performance.

TABLE I

Photovoltaic Module Specifications

Datasheet	I_{sc}	V_{oc}	I_{op}	V_{op}	b
Siemens SP75	$4.80A$	$21.7V$	$4.40A$	$17.0V$	0.08717
Shell SQ80	$4.85A$	$21.8V$	$4.58A$	$17.5V$	0.06829
SLK60M6	$7.52A$	$37.2V$	$6.86A$	$30.6V$	0.07292
Solarex SA-5	$0.38A$	$25.0V$	$0.34A$	$15.0V$	0.13900

TABLE II

Photovoltaic Module Specifications (cont.)

Datasheet	TCi	TCV	V_{min}	V_{max}
Siemens SP75	$2.06mA/^{\circ}C$	$-77mV/^{\circ}C$	$18.45V$	$22.243V$
Shell SQ80	$1.4mA/^{\circ}C$	$-81mV/^{\circ}C$	$20.25V$	$21.810V$
SLK60M6	$2.2mA/^{\circ}C$	$-127mV/^{\circ}C$	$32.55V$	$37.312V$
Solarex SA-5	$0.3mA/^{\circ}C$	$-60mV/^{\circ}C$	$21.00V$	$25.500V$

TABLE III

Measured Values for *Algorithm 1*

Datasheet	I_1	V_1	Vx	E_i	T
Siemens SP75	$3.00A$	$18.0V$	$19.8V$	$1,000W/m^2$	$45^{\circ}C$
Shell SQ80	$3.62A$	$16.0V$	$20.0V$	$800W/m^2$	$46^{\circ}C$
SLK60M6	$8.20A$	$10.0V$	$35.0V$	$1,100W/m^2$	$50^{\circ}C$
Solarex SA-5	$0.28A$	$19.5V$	$25.3V$	$1,000W/m^2$	$20^{\circ}C$

TABLE IV

Calculated Values using *Algorithm 1*

Datasheet	$Iterations(n)$	$E_i(Appr.)$	$T(Appr.)$
Siemens SP75	5	$955.7W/m^2$	$47.976^{\circ}C$
Shell SQ80	4	$785.7W/m^2$	$42.271^{\circ}C$
SLK60M6	4	$1,084W/m^2$	$44.045^{\circ}C$
Solarex SA-5	4	$966.5W/m^2$	$19.552^{\circ}C$

TABLE V

Measured Values for *Algorithm 2*

Datasheet	I_1	V_1	Vx	E_i	T
Siemens SP75	$3.00A$	$18.0V$	$19.8V$	$1,000W/m^2$	$45^{\circ}C$
Shell SQ80	$3.62A$	$16.0V$	$20.0V$	$800W/m^2$	$46^{\circ}C$
SLK60M6	$8.20A$	$10.0V$	$35.0V$	$1,100W/m^2$	$50^{\circ}C$
Solarex SA-5	$0.28A$	$19.5V$	$25.3V$	$1,000W/m^2$	$20^{\circ}C$

TABLE VI

Calculated Values using *Algorithm 2*

Datasheet	$Iterations(n)$	$E_i(Appr.)$	$T(Appr.)$	Pap
Siemens SP75	5	$795.4W/m^2$	$44.980^{\circ}C$	$64.7W$
Shell SQ80	4	$810.3W/m^2$	$42.845^{\circ}C$	$60.9W$
SLK60M6	4	$794.7W/m^2$	$39.204^{\circ}C$	$162W$
Solarex SA-5	4	$1,015W/m^2$	$72.656^{\circ}C$	$5.12W$

V. Conclusions

Several algorithms have been presented, which are capable of calculating the effective irradiance level and temperature over a PVM. The proposed algorithms eliminate the use of thermocouples and pyranometers, reducing the cost and

complexity of a PV power system. These algorithms have several advantages such as being easy to execute and very efficient using the data of operation provided by the PVM and having very fast convergence. Three of the algorithms use only the data provided by the voltage sensor and current sensor, which is excellent to track changes in the temperature and irradiance level in a geographic region over long periods of time. These algorithms can be integrated to MPPT and other monitoring algorithms, and can be implemented in RT Linux or a fast controller like a DSP. The algorithms have high accuracy (3%), working as a high cost pyranometer but without paying the high price and like an integrated thermocouple without affect the PV power system performance. Finally, these algorithms are well suited for monitoring in remote areas, especially in developed countries where not always the economic infrastructure is available.

REFERENCES

[1] T.F. El Shatter and M.T. Elhagry. Sensitivity analysis of the photovoltaic model parameters. In *Midwest Symposium on Circuits and Systems*, pages 914–917, 1999.

[2] R. Gottschalg, M. Rommel, D.G. Infield, and M. J. Kearney. The influence of the measurement environment on the accuracy of the extraction of the physical parameters of solar cells. In *Measurement Science and Technology*, pages 797–804, 1999.

[3] D.L. King, W.E. Boyson, and P. Kratochvil. Analysis of factors influencing the annual energy production of photovoltaic systems. In *IEEE Photovoltaic Specialists Conference*, pages 1356–1361, 2002.

[4] G. Batsukh, D. Ochirbaani, C. Lkhagvajav, N. Enebish, B. Ganbat, T. Baatarchuluun, K. Otani, and K. Sakuta. Evaluation of solar energy potentials in Gobi desert area of Mongolia. In *World Conference on Photovoltaic Energy Conversion*, pages 2262–2264, 2003.

[5] M.W. Davis, A.H. Fanney, and B.P. Dougherty. Evaluating building integrated photovoltaic performance models. In *IEEE Photovoltaic Specialists Conference*, pages 1642–1645, 2002.

[6] M.A. Abella, E. Lorenzo, and F. Chenlo. Effective irradiance estimation for PV applications. In *World Conference on Photovoltaic Energy Conversion*, pages 2085–2089, 2003.

[7] Bureau of Meteorology, Commonwealth of Australia. *Solar Radiation Definitions*, 2006.

[8] F. Chenlo, N. Vela, and J. Olivares. Comparison between pyranometers and encapsulated solar cells as reference PV sensors-outdoor measurements in real conditions. In *IEEE Photovoltaic Specialists Conference*, pages 1099–1104, 1990.

[9] D.L. King, W.E. Boyson, B.R. Hansen, and W.I. Bower. Improved accuracy for low-cost solar irradiance sensors. In *Photovoltaic Solar Energy Conversion*, pages 1947–1952, 1998.

[10] A. Hunter Fanney, B.P. Dougherty, and M.W. Davis. Performance and characterization of building integrated photovoltaic panels. In *IEEE Photovoltaic Specialists Conference*, pages 1493–1496, 2002.

[11] The University of Georgia, Giffin, GA. *Georgia Solar Radiation Database*, 2006.

[12] Today's Solar Radiation for Austin, Texas, 2006.

[13] C.J. Van Dan Bos and A. Van Dan Bos. Solar radiation sensors: applications, new detector development, characterization and classification according to ISO 9060. In *IEEE Instrumentation and Measurement Technology Conference*, pages 175–178, 1995.

[14] D.L. King, J.A. Kratochvil, and W.E. Boyson. Temperature coefficients for PV modules and arrays: measurement methods, difficulties, and results. In *IEEE Photovoltaic Specialists Conference*, pages 1183–1186, April 1999.

[15] Pico Technology Limited. Thermocouple Application Note. Technical report, Pico Technology Limited.

[16] E.I. Ortiz-Rivera and F.Z. Peng. A novel method to estimate the maximum power for a photovoltaic inverter system. In *Power Electronics Specialists Conference*, volume 3, pages 2065–2069, 2004.

[17] E. I. Ortiz-Rivera and F.Z. Peng. Analytical Model for a Photovoltaic Module using the Electrical Characteristics provided by the Manufacturer Data Sheet. In *Power Electronics Specialists Conference*, pages 2087–2091, June 2005.

[18] D. R. Smart. *Fixed Point Theorems*. Cambridge University Press, 1974.

[19] W. Rakowski. The fixed point theorem in computing magnetostatic fields in a nonlinear medium. *IEEE Trans. Magnetics*, 18:391–392, March 1982.

[20] V. Mainkar and K.S. Trivedi. Sufficient conditions for existence of a fixed point in stochasticreward net-based iterative models. *IEEE Trans. Software Engineering*, 22(9):640–653, September 1996.